American Journal of Pathology, Vol. 168, No. 5, May 2006
Copyright © American Society for Investigative Pathology
DOI: 10.2353/ajpath.2006.050865

Immunopathology and Infectious Diseases

Ongoing Coxsackievirus Myocarditis Is Associated with Increased Formation and Activity of Myocardial Immunoproteasomes

Gudrun Szalay,* Silke Meiners,† Antje Voigt,†‡ Jörg Lauber,§ Christian Spieth,¶ Nora Speer,¶ Martina Sauter,* Ulrike Kuckelkorn,‡ Andreas Zell,¶ Karin Klingel,* Karl Stangl,† and Reinhard Kandolf*

From the Department of Molecular Pathology, University Hospital Tübingen, Tübingen; Clinic for Cardiology, Angiology, and Pneumology,† and Institute of Biochemistry,‡ Charité-Universitätsmedizin, Berlin; the German Research Center for Biotechnology,§ Braunschweig; and the Center for Bioinformatics Tübingen, Eberhard-Karls-University,¶ Tübingen, Germany*

A growing body of evidence indicates that viral infections of the heart contribute to ongoing myocarditis and dilated cardiomyopathy. Murine models of coxsackievirus B3 (CVB3)-induced myocarditis mimic the human disease and allow identification of susceptibility factors that modulate the course of viral myocarditis. Susceptible mouse strains develop chronic myocarditis on the basis of restricted viral replication, whereas resistant strains recover after successful virus elimination. In comparative whole-genome microarray analyses of infected hearts, several genes involved in the processing and presentation of viral epitopes were found to be uniformly up-regulated in acutely CVB3-infected susceptible mice compared with resistant animals. In particular, expression of the catalytic subunits LMP2, LMP7, and MECL-1, immunoproteasome proteins important in the generation of major histocompatibility complex (MHC) class I-restricted peptides, was clearly enhanced in the susceptible host. Increased expression resulted in enhanced formation of immunoproteasomes and altered proteolytic activities of proteasomes in the heart. This was accompanied by a concerted up-regulation of the antigen-presenting machinery in susceptible mice. Thus, we propose that increased formation of immunoproteasomes in susceptible mice affects the generation of antigenic peptides and the subsequent T-cell-mediated immune responses. ***(Am J Pathol 2006, 168:1542–1552; DOI: 10.2353/ajpath.2006.050865)***

Viral infections of the heart, which may produce acute myocarditis, have been increasingly associated with the development of dilated cardiomyopathy (DCM) due to the presence of viral nucleic acids and proteins and possibly chronic inflammatory processes.[1] A recent study has reported cardiac viral infections in a majority of patients with sporadic DCM.[2] Cardiotropic viruses thus emerge as prevalent environmental factors that appear to cause or modulate the course of DCM. The progression of cardiac viral infections depends strongly on genetic host factors and may range from rapid and complete virus elimination or silencing without clinical symptoms to rapidly progressive or fatal disease. Thus, the identification of susceptibility factors affecting the course of viral infection in humans is of central clinical importance to improve diagnosis and prognosis of myocarditis and DCM.

Coxsackievirus B3 (CVB3) infections are one of the most frequent causes of human myocarditis.[3] Although the majority of infections are subclinical, CVB3 infection can produce severe acute myocarditis and may lead to ongoing myocarditis and DCM.[4] Murine models of CVB3-induced myocarditis mimic the human disease process, providing a unique opportunity to define the involvement of host factors that determine the course of disease. Susceptible mouse strains, like A.BY/SnJ and SWR/J mice, develop ongoing myocarditis after acute infection due to the presence of viral RNA and the restricted synthesis of viral proteins after acute infection; resistant C57BL/6 and DBA/1J mouse strains, however, eliminate the virus after acute infection.[5] The chronic course of disease points to evasion

Supported by grants from the Federal Ministry of Education, Science, Research, and Technology (BMBF) within the National Genome Research Network (grant no. 01GS0114 to G.S. and R.K.) and the Deutsche Forschungsgemeinschaft (SFB/TR 19–04 "Inflammatory Cardiomyopathy" B3 to K.S. and U.K. and B4 to K.K.).

G.S., S.M., and A.V. contributed equally to this work.

Accepted for publication January 12, 2006.

Address reprint requests to Dr. Gudrun Szalay, Department of Molecular Pathology, University Hospital Tübingen, Liebermeisterstrasse 8, D-72076 Tübingen, Germany. E-mail: gnszalay@med.uni-tuebingen.de.

of CVB3 from immunological surveillance. Experiments with immune-deficient mice have revealed that both humoral and cellular immune responses are necessary to control CVB3 infection.[6–8] In T-cell-mediated immunity, CD4 as well as CD8 T-cell subsets play a protective role.[9,10] The importance of CD8 T-cell responses in CVB3 myocarditis has been demonstrated by analysis of CVB3-infected β_2-microglobulin gene-deleted ($\beta_2 m^{-/-}$) mice, perforin gene-deleted (*perforin*$^{-/-}$) mice, fas-deficient *lpr/lpr* mice, and CD8 T-cell-depleted CD4 gene-deficient mice.[9,11–13] The studies of CVB3 infection of $\beta 2m^{-/-}$ mice and perforin$^{-/-}$ mice have underlined a preponderant role of cytokines produced by CD8 T cells in protection against ongoing myocarditis in comparison with the direct cytolytic action of virus-specific CD8 T cells.[11]

In antiviral immunity mediated by CD8 T cells, specific recognition of viral antigens presented by MHC class I molecules is crucial for virus elimination.[14] Antigenic peptides are generated by proteases involved in the turnover and degradation of cellular and viral proteins.[15] Among these proteases, the proteasome is essential for the generation of most MHC class I-restricted antigenic peptides. For degradation, proteins are first covalently tagged with multiubiquitin chains and then targeted to the 26S proteasome, which consists of a 20S catalytic core complex and two 19S regulatory complexes. The 20S catalytic core is composed of 14 nonidentical subunits building four stacked rings of seven subunits each. Seven different but related α subunits form the two outer rings, whereas the two inner rings contain seven different β subunits. The hydrolyzing activities of the 20S core reside in three of the seven β subunits, ie, β_1, β_2, and β_5, located in both of the two inner rings.[16] Proteasomal processing results in the generation of small peptides that are transported via transporter-associated proteins (TAPs) into the endoplasmic reticulum, where they are loaded onto MHC class I molecules. MHC class I molecules at the cell surface then present these antigenic peptides to CD8 T cells. On stimulation of cells with inflammatory cytokines, namely interferon-γ, the three catalytic β subunits are replaced by their inducible counterparts LMP2, LMP7, and MECL-1, thus forming the so-called immunoproteasome.[17] This newly assembled immunoproteasome has an altered cleavage site preference and a different protein cleavage rate, resulting in enhanced generation of antigenic peptides. Thus, immunoproteasome activity influences T-cell selection by changing the relative prevalence by which epitopes are presented on the cell surface.[18]

The present study was undertaken to analyze tissue-specific host factors that might influence the course of CVB3 myocarditis in susceptible and resistant mouse strains. In infected hearts, we identified several genes involved in the processing and presentation of viral epitopes that were more strongly up-regulated in CVB3-infected susceptible mice compared with resistant animals. In particular, increased expression of immunoproteasomal subunits LMP2, LMP7, and MECL-1 resulted in enhanced formation of immunoproteasomes and altered proteolytic activities of cardiac proteasomes. This was accompanied by a concerted up-regulation of the antigen-presenting machinery, namely TAP and MHC class I molecules in susceptible mice. Surprisingly, enhanced up-regulation of the antigen-processing and -presenting machinery in susceptible mice did not lead to efficient virus elimination but resulted in the development of ongoing myocarditis. We propose that increased generation of immunoproteasomes affects the generation of antigenic peptides and alters the T-cell-mediated immune responses to CVB3 epitopes in susceptible mice.

Materials and Methods

Virus and Mice

CVB3 used in this study was derived from the infectious cDNA copy of the cardiotropic Nancy strain, and virus stocks were prepared as described previously.[19] Immunocompetent inbred mice [strains C57BL/6 (H-2^b), A.BY/SnJ (H-2^b), DBA/1J (H-2^q), and SWR/J (H-2^q)] were kept under specific pathogen-free conditions at the animal facilities of the Department of Molecular Pathology, University Hospital Tuebingen, and experiments were conducted according to the German animal protection law. Four- to 5-week-old mice were infected intraperitoneally with 1×10^5 plaque-forming units of purified CVB3 as described previously.[5] At days 4, 8, and 28 post infection (p.i.), mice were anesthetized, and hearts were perfused with phosphate-buffered saline and removed for analysis.

Determination of Virus Load

The viral load of hearts from infected mice ($n = 9$) was determined as previously described.[11] $TCID_{50}$, defined as the dilution required to infect 50% of inoculated wells, was determined by the method of Reed-Muench and is expressed as $TCID_{50}$ per milligram of cardiac tissue.

Pooling of Probes and Statistical Analysis

For RNA experiments, isolated RNA of five individual mice of every mouse strain, either infected or uninfected, was pooled in equal amounts to normalize individual variations of gene expression in the mouse strains. In first experiments for real-time reverse transcriptase-polymerase chain reaction (RT-PCR), we investigated individual RNAs in comparison with pooled RNA of one mouse strain to obtain information on the individual variation of expression levels. Because the expression variations of individual RNAs within one mouse strain were minimal and the mean values similar to pooled RNA, we decided to use pooled RNA for our experiments. To obtain sufficient material for the elaborate purification procedure of 20S proteasome, we pooled protein extracts from 10 hearts of uninfected or CVB3-infected mouse strains, thereby normalizing the variation in proteasome composition of individual mice. For this reason, we did not apply statistical analysis on the real-time RT-PCR, Western blot, two-dimensional (2-D) gel, or activity measurements. However, we repeated all experiments twice to ensure

reproducibility of our results. When statistical analysis was performed, data are expressed as means ± SD. Significance was calculated by use of Mann-Whitney *U*-test using SPSS 11.0 software. An error probability of $p < 0.05$ was regarded as significant.

DNA Microarray Hybridization and Analysis

Total RNA of murine heart tissue was isolated by using Trizol reagent (Invitrogen, Karlsruhe, Germany) followed by the RNeasy Mini Kit (Qiagen, Duesseldorf, Germany). RNA of five animals was pooled in equal amounts, and 5 μg of total RNA was used for biotin-labeled cDNA synthesis. RNA was converted to cDNA using 100 pmol of a T7T23V primer (Eurogentec, Cologne, Germany) containing a T7 promoter. The cDNA was used in *in vitro* transcription reactions in the presence of biotinylated nucleotides. A portion of the resulting cRNA (12.5 μg) was fragmented and used for hybridization to an identical lot of MG-U74Av2 chips (Affymetrix, Santa Clara, CA). Data analysis was performed with gene expression software supplied by Affymetrix (GeneChip, MicroDB, and Data Mining Tool). For normalization, all experiments were scaled to a target intensity of 150. The filter for regulated genes was fold changes >2 or <−2 and change *p* values $p < 0.001$ or $p > 0.999$.

Real-Time RT-PCR

RNA isolated for the microarray analysis was used for real-time RT-PCR. RNA (500 ng) was digested with DNase (Ambion, Huntingdon, UK) and reverse-transcribed with molony murine leukemia virus reverse transcriptase (Invitrogen). The PCR primers to amplify cDNA of mouse proteasome LMP7 (*PSMB8*), LMP2 (*PSBM9*), MECL-1 (*PSMB10*), and α5 (*PSMA5*) and the housekeeping gene hypoxanthine phosphoribosyl transferase (*HPRT*) were purchased from TIB MOLBIOL (Berlin, Germany). The SYBR Green method was applied for quantitative amplification of the cDNAs as described previously.[20] Briefly, PCR amplification was performed in 25 μl of TaqMan Universal PCR Master Mix (Perkin Elmer/Applied Biosystems, Lincoln, CA) containing either 0.3 or 0.9 μmol/L primer and 0.4 μl of the reverse transcription reaction in a 5700 Sequence Detection System (Perkin Elmer/Applied Biosystems). Thermal cycling conditions comprised activation of uracil-*N*-glycosylase at 50°C for 2 minutes and an initial denaturation step at 95°C for 10 minutes, followed by 95°C for 15 seconds and 60°C for 1 minute for 40 cycles. The threshold cycle (C_T) is defined as the number of cycles required for the fluorescence signal to exceed the detection threshold. The mRNA expression was standardized to *HPRT* gene as a housekeeping gene by means of the ΔC_T method. Expression of immunoproteasomal subunits in infected animals was normalized to expression in noninfected controls using the comparative C_t method ($2^{-\Delta\Delta Ct}$).

List of Primers Used

Mouse α5 forward, 5′-CGCTCATCATCCTCAAGCAAG-3′; mouse α5 reverse, 5′-AAATTCTGACCAGGCTGCA-CC-3′; mouse LMP7 forward, 5′-TGCTTATGCTACCCA-CAGAGACAA-3′; mouse LMP7 reverse, 5′-TCCACTT-TCACCCAACCGTC-3′; mouse LMP2 forward, 5′-GTTCT-GGCTGCTGCAAACGT-3′; mouse LMP2 reverse, 5′-GTCCCAGCCAGCTACTATGAGATG-3′; mouse MECL-1 forward, 5′-GAAGACCGGTTCCAGCCAA-3′; mouse MECL-1 reverse, 5′-CACTCAGGATCCCTGCTGTGAT-3′; mouse HPRT forward, 5′-TGAAGGAGATGGGAGGCCA-3′; and mouse HPRT reverse, 5′-AATCCAGCAGGTC-AGA-3′.

In Situ *Hybridization*

CVB3 positive-strand genomic RNA in tissues was detected using single-stranded ^{35}S-labeled RNA probes that were synthesized from the dual-promoter plasmid pCVB3-R1.[5] Control RNA probes were obtained from the vector pSPT18. ^{35}S-labeled antisense and sense RNA probes for detection of LMP7 were synthesized by *in vitro* transcription from the dual-promoter plasmid pTOPO-LMP7 containing an 828-bp murine cDNA fragment. Pretreatment, hybridization, and washing conditions of dewaxed 5-μm paraffin tissue sections were performed as described previously.[5] Slide preparations were subjected to autoradiography, exposed for 3 weeks at 4°C and counterstained with hematoxylin and eosin. LMP7 mRNA content at the single cell level was determined by counting silver grains in $n = 50$ cells per mouse strain. For quantitative comparison of CVB3 RNA content in myocytes, heart tissue slides were autoradiographed for only 4 days, and grains were counted ($n = 50$ cells per mouse strain).

Cell Lysate Generation and Proteasome Purification

Ten hearts of infected mice or uninfected controls were pooled, minced in liquid nitrogen, and lysed in H_2O containing a protease-inhibitor cocktail (Complete; Roche Molecular Biochemicals, Mannheim, Germany) under hypo-osmotic conditions by repeated freezing and thawing. 20S proteasomes were isolated by diluting the lysate with lysis buffer containing 20 mmol/L Tris, pH 7.2, 1 mmol/L ethylenediamine tetraacetic acid, 1 mmol/L NaN_3, 1 mmol/L dithiothreitol, 0.1% NP-40 supplemented with 2 μmol/L pepstatin, 2 μmol/L bestatin, and protease-inhibitor cocktail. Filtered lysates were applied onto DEAE Sephacel (Amersham Pharmacia Biotech, Freiburg, Germany) and carefully washed with 50 and 150 mmol/L NaCl until no protein was detected by UV absorption (280 nm). Proteasomes were eluted with 400 mmol/L NaCl in TEAD (20 mmol/L **T**ris-HCl [pH 7.2], 1 mmol/L **e**thylenediamine tetraacetic **a**cid, 1 mmol/L NaN_3, and 1 mmol/L dithioerythrit) buffer and concentrated by ammonium sulfate precipitation between 40 and 70% saturation. Protein frac-

tions were separated by ultracentrifugation on sucrose gradients (10 to 40%) and ultracentrifuged at 40,000 rpm for 16 hours in a Beckman Coulter SW40 rotor (Beckman, Krefeld, Germany). Fractions containing proteasomes were pooled and applied to a MonoQ column (FPLC; Amersham Pharmacia Biotech, Munich, Germany) and eluted with a linear gradient of 100 to 500 mmol/L NaCl in TEAD. 20S proteasome purification was performed twice in two different animal experiments.

Western Blot Analysis

To identify immunoproteasome subunit protein expression, protein extracts of isolated myocardial 20S proteasomes were separated by sodium dodecyl sulfate-polyacrylamide gel electrophoresis (SDS-PAGE) in 15% polyacrylamide gels, and Western blots were performed following standard procedures.[21] Antibodies used for specific detection included K464/A for LMP2 subunit, K63/5 for LMP7 subunit, K65/4 for MECL-1 subunit, and K379 for α6 subunit. Proteasomes of the human lymphoblastoid B-cell-derived T2 cell line and the T2 transfectant T27mp, which expresses mouse proteasome subunits LMP2, LMP7, and MECL-1, served as negative and positive controls, respectively.

Two-Dimensional Mini-Gelelectrophoresis and Spot Identification by Mass Spectroscopy

For resolution of 20S proteasome proteins, we combined isoelectric focusing by carrier ampholytes with SDS-PAGE.[22] We applied 5 μg of protein to the anodic side of a carrier ampholyte isoelectric focusing (IEF) gel. In the second dimension, proteins were separated in 0.75-mm-thick 15% SDS-PAGE gels (7 $\times$ 8 cm) followed by silver staining.[23] Individual spots were excised, digested by trypsin, desalted and concentrated by ZIPTIP, and analyzed by matrix-assisted laser desorption-ionization mass spectrometry as described recently.[24]

Measurement of Proteasome Activity

Proteolytic activities of the 20S proteasomes of CVB3-infected pooled heart tissues and controls were assessed using synthetic peptides linked to the fluorometric reporter aminomethylcoumarin (AMC) as described previously.[20] For the determination of chymotrypic-like activity, the peptide S-LLVY-AMC was used; Z-LLE-AMC for caspase-like and BzVGR-AMC for tryptic-like activity. 20S proteasomes (300 ng) were incubated for 30 minutes at 37°C in incubation buffer (50 mmol/L Tris-HCl, pH 8.2, 10 mmol/L $Mg(CH_3COO)_2$, and 1 mmol/L dithiothreitol) and 0.2 mmol/L substrate. Release of the fluorometric reporter AMC was quantitated in a Spectra MAX Gemini EM plate reader (Molecular Device, Munich, Germany) using 370-nm excitation and 445-nm emission wavelengths.

Results

Enhanced Expression of Genes Involved in Antigen Processing and Presentation in Susceptible Mice during Acute Infection with CVB3

In an attempt to identify differential gene expression patterns associated with different courses of CVB3 myocarditis, we performed whole-genome microarray analyses. For this purpose, we isolated RNA from hearts of noninfected and CVB3-infected susceptible (ABY/SnJ and SWR/J) and resistant (C57BL/6 and DBA1/J) mouse strains at different time points after infection (early [day 4 p.i.], acute [day 8 p.i.], and chronic [day 28 p.i.] stages of disease). To exclude haplotype-specific expressional regulation in response to CVB3 infection, we used susceptible and resistant mouse strains with two different MHC haplotypes, namely H-2^b (ABY/SnJ and C57BL/6) and H-2^q (SWR/J and DBA1/J). When we examined differential gene expression of CVB3-infected susceptible and resistant animals compared with noninfected controls irrespective of the infection phase, a uniform pattern emerged with increased expression of several genes involved in antigen processing and presentation in susceptible mice (Table 1, see highlighted genes). In particular, we observed concerted up-regulation of the three catalytic subunits of the immunoproteasome, LMP2, LMP7, and MECL-1, and increased expression of antigenic peptide transporter (Abcb2, synonym for TAPb2) and several MHC class I molecules like H2-D, H2-K, or H2-T. Hence, we analyzed cardiac expression of these genes in susceptible and resistant mice at different time points after CVB3 infection in detail. As summarized in Figure 1, investigations of different phases of infection by microarray (left panel) and real-time RT-PCR (right panel) analysis revealed that as early as day 4 p.i., all three immunoproteasomal subunits, LMP7, LMP2, and MECL-1, were uniformly up-regulated on CVB3 infection in all four mouse strains. However, in the acute phase (day 8 p.i.), expression of LMP7, LMP2, and MECL-1 was clearly enhanced in susceptible A.BY/SnJ and SWR/J mice compared with resistant C57BL/6 and DBA/1J mice. Calculated from the quantitative PCR data, the differences in immunoproteasome expression between susceptible and resistant mouse strains within the two haplotypes H-2^b (A.BY/SnJ; C57BL/6) and H-2^q (SWR/J; DBA/1J) ranged from 2.5- to 5.5-fold up-regulation for LMP7 and MECL-1, respectively. During the chronic phase of myocarditis (day 28 p.i.), LMP7, LMP2, and MECL-1 expression was only slightly increased, irrespective whether CVB3 was persistent (A.BY/SnJ, SWR/J) or was eliminated (C57BL/6, DBA/1J) from the myocardium. Similarly, enhanced cardiac gene expression of classical and nonclassical MHC class I, β2-microglobulin, TAP, and tapasin (a component of the class I peptide-loading system) was observed during the acute phase of infection. The ratio of fold changes of these genes between susceptible and resistant mice was in every case higher in susceptible mice, varying from 1.4- to 2.9-fold (Table

Table 1. Differentially Expressed Genes in Hearts of CVB3-Infected Susceptible (A.BY/SnJ; SWR/J) and Resistant (C57BL/6; DBA1/J) Mouse Strains versus Noninfected Controls

	Susceptible mouse strains		Resistant mouse strains	
No.	Gene	Fold change	Gene	Fold change
1	*AW558444*	7.4	*Ifit1*	10.1
2	*Tgtp*	6.0	*Ifit3*	7.7
3	*Apod*	5.8	*Ifit2*	5.5
4	*Gtpi-pendi*	5.7	*AW558444*	5.5
5	*Ifit2*	5.4	*Apod*	5.1
6	*Iigp-pendi*	5.2	*AI046432*	3.9
7	*Gbp3*	4.7	*Gtpi-pendi*	3.8
8	*NULL*	4.4	*Ifi1*	3.8
9	*AI046432*	4.3	*Iigp-pendi*	3.3
10	*Igk-V28*	4.2	*Gbp3*	3.2
11	*Stat1*	4.0	*Tgtp*	3.2
12	***H2-Q2***	**4.0**	***H2-T17***	**3.1**
13	***LMP2***	**3.8**	*4921504P20*	3.1
14	***LMP7***	**3.8**	***H2-D1***	**2.9**
15	***H2-T17***	**3.7**	***H2-T10***	**2.8**
16	*C4*	3.5	LOC56628	2.7
17	***H2-D1***	**3.4**	***H2-Q7***	**2.7**
28	***Abcb2***	**3.1**	*Stat1*	**2.7**
19	*4921504P20*	3.1	*1110013J02*	2.6
20	***H2-T10***	**3.1**	***LMP7***	**2.6**
21	***H2-Q7***	**3.0**	***H2-K***	**2.5**
22	***MECL-1***	**2.9**	*Cd52*	2.5
23	***H2-K***	**2.9**	*C4*	2.4
24	***H2-T23***	**2.8**	*Xdh*	2.4
25	*Ctss*	2.8	*2010008K16*	2.3
26	*Cd53*	2.8	*Ctss*	2.3
27	*Gbp2*	2.8	***H2-L***	**2.3**
28	*1110013J02*	2.6	*NULL*	2.3
29	*Gp49a*	2.4	***H2-D1***	**2.2**
30	*C3*	2.4	***ß2-microglobulin***	**2.2**
31	***ß2-microglobulin***	**2.3**	*Ppicap*	2.2
32	***H2-L***	**2.3**	***Abcb2***	**2.2**
33	*Ppicap*	2.2	*Ifi202a*	2.2
34	*Ifi204*	2.1	*Ddit3*	2.1
35	*2010008K16*	2.1	*NULL*	2.1
36	*1910027D10*	2.1	*Mt2*	2.1
37	*Mt2*	2.1	***LMP2***	**2.1**
38	*NULL*	2.0	*Ifi204*	2.0
39	*Vcam*	2.0	*Myhcb*	2.0
40	***H2-Bl***	**2.0**	***MECL-1***	**2.0**

The values are given as the fold change of genes in CVB3-infected susceptible or resistant mouse strains versus uninfected controls irrespective of infection phase. The cut-off for regulated genes was fold changes >2 or <−2 and change p values $p < 0.001$ or $p > 0.999$.

2). Detailed analysis of the time course of immunoproteasome expression during CVB3 myocarditis revealed that the highest expression was detected at day 8 p.i. and was reduced to uninfected control levels in resistant C57BL/6 mice by day 10 p.i. (Figure 2). In susceptible A.BY/SnJ mice, expression levels of LMP2, LMP7, and MECL-1 were still slightly elevated at day 10 and were almost completely reduced to uninfected control levels at day 12 p.i., indicating that immunoproteasome up-regulation is not an incidental observation on a single day but has relevance for ongoing myocarditis.

Our data suggest that CVB3-infected susceptible mice up-regulate expression of the antigen-processing and -presenting machinery in a concerted manner during the acute phase of CVB3 infection compared with resistant mice. Importantly, this up-regulation occurs irrespective of the MHC haplotype of the mouse strain, indicating a general, MHC-independent mechanism for the development of ongoing myocarditis in the heart of susceptible animals. Because the generation of antigenic peptides by the proteasome is the rate-limiting step in MHC class I-restricted antigen presentation, we focused on the detailed investigation of immunoproteasome expression for further analysis.[25]

Increased Expression of LMP7 in Cardiomyocytes and Infiltrating Cells of Susceptible Mice

To identify the cells that contribute to the elevated expression levels of immunoproteasome subunits in CVB3-infected hearts of susceptible animals, we performed *in situ* hybridization experiments with specific RNA probes for the murine immunosubunit LMP7. We chose LMP7 as a representative gene for immunoproteasome expression for two reasons: first, this subunit replaces the constitutive β5 subunit, which forms the main proteolytic activity

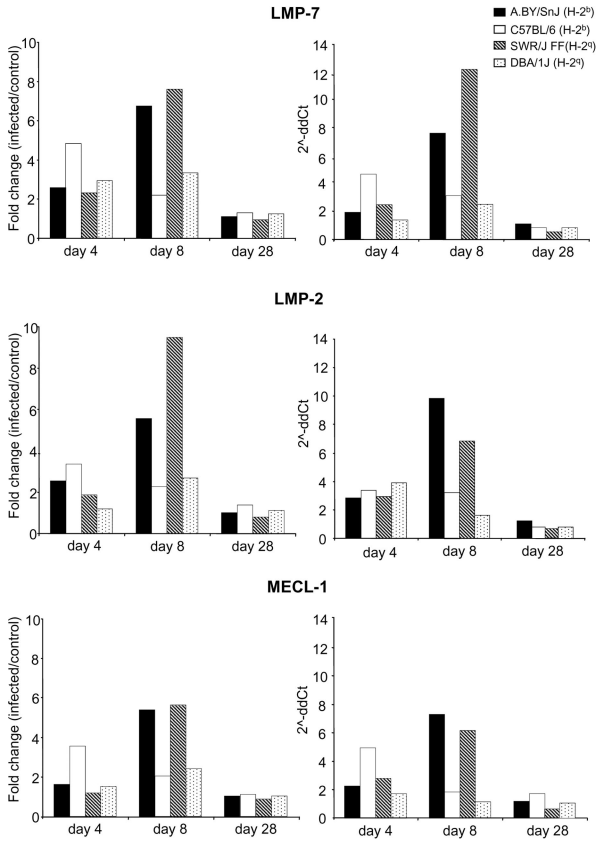

Figure 1. Regulation of LMP7, LMP2, and MECL-1 expression in the course of CVB3 myocarditis. Comparison of changes in immunosubunit expression of CVB3-infected mice and uninfected controls at days 4, 8, and 28 p.i. obtained by microarray analysis (**left**) and quantitative PCR analysis (**right**). At day 8 p.i., the strongest up-regulation of LMP7, LMP2, and MECL-1 was detected in susceptible mice (A.BY/SnJ, SWR/J) compared with resistant mice (C57BL/6, DBA/1J). At days 4 and 28 p.i., up-regulation was less pronounced and nearly uniform in all four mouse strains. RNA was pooled from five animals per mouse strain, and experiments were repeated twice.

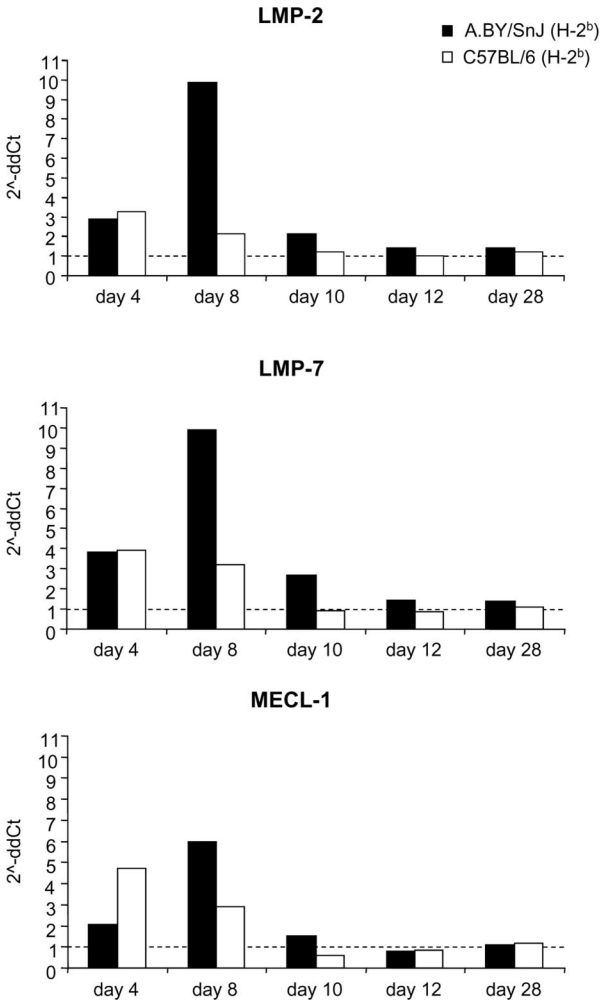

Figure 2. Time course of immunoproteasome expression in CVB3-infected susceptible and resistant mice. Quantitative RT-PCR analysis of expression of LMP7, LMP2, and MECL-1 at days 4, 8, 10, 12, and 28 p.i. revealed that the enhanced up-regulation in A.BY mice is prolonged up to day 10 p.i. compared with resistant C57BL/6 mice. At days 12 and 28 p.i., both mouse strains show expression levels of LMP7, LMP2, and MECL-1 that are similar to uninfected controls, as indicated by the **dashed line**. RNA was pooled from five animals per mouse strain, and experiments were repeated twice. Expression of immunoproteasomal subunits in infected animals was normalized to expression in noninfected controls by means of the comparative C_t method ($2^{-\Delta\Delta Ct}$).

of the proteasome; second, LMP7 is essential for proper assembly and maturation of immunoproteasomes.[26] To monitor CVB3 infection in parallel, an enterovirus-specific RNA probe was used. We examined heart tissue from A.BY/SnJ mice and C57BL/6 mice at day 8 p.i., because

Table 2. Increased Expression of MHC Class I and TAP Genes in Infected Susceptible Mice Compared with Infected Resistant Mice during the Acute Phase of CVB3 Infection (day 8 p.i.) in the Heart

Gene	Fold change in susceptible mice (infected versus control)	Fold change in resistant mice (infected versus control)	Ratio of fold change (susceptible versus resistant mice)
H2-Q2	6.4 ± 0.9	2.2 ± 0.01	2.9
TAP transporter b2	6.2 ± 1.4	2.4 ± 0.2	2.6
TAP transporter b3	2.6 ± 0.3	1.0 ± 0.3	2.6
H2-T10	5 ± 1.2	2.0 ± 0.03	2.5
H2-T23	4.2 ± 0.5	1.7 ± 0.03	2.5
H2-T17	5.7 ± 0.6	2.5 ± 0.06	2.3
Tapasin	2.3 ± 0.1	1.0 ± 0.03	2.3
H2-D1	5.6 ± 0.1	3.2 ± 0.42	1.8
H2-Q7	4.6 ± 0.2	2.6 ± 0.2	1.8
H2-L	4.5 ± 0.3	2.4 ± 0.03	1.8
H2-K	4.6 ± 0.1	2.7 ± 0.1	1.7
ß2-microglobulin	3.2 ± 0.0	2.3 ± 0.4	1.4

The values are given as the mean of two independent array experiments for two susceptible (A.BY/SnJ; SWR/J) and resistant (C57BL/6; DBA/1J) mouse strains ± SD.

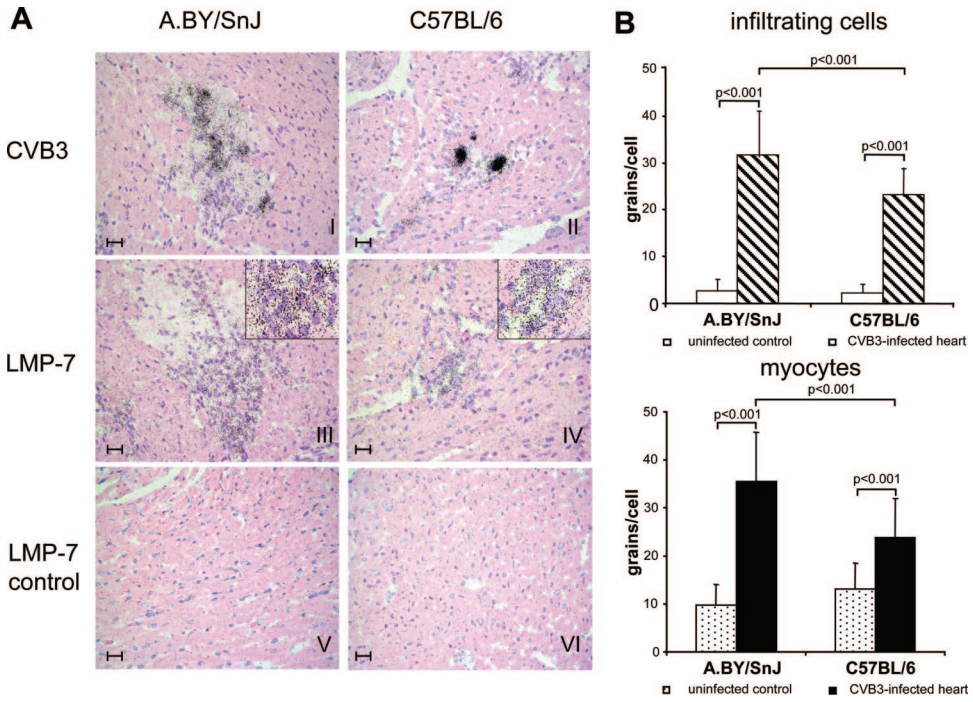

Figure 3. Identification and quantification of LMP7 mRNA-expressing cells in the myocardium of CVB3-infected susceptible (A.BY/SnJ) and resistant (C57BL/6) mice by *in situ* hybridization. **A:** CVB3 infection is more pronounced in A.BY/SnJ mice (I) compared with C57BL/6 mice at day 8 p.i. (II). Increased LMP7 expression in cardiomyocytes of infected animals compared with uninfected controls (III and V and IV and VI) and in infiltrating cells (3A III and IV, **inset**) of infected animals. Bars = 20 μm. **B:** Quantification of LMP7-specific silver grains in single cardiomyocytes and infiltrating cells ($n = 50 \pm$ SD, p values were determined by Mann-Whitney U-test).

this time point represents the peak of CVB3 replication in the myocardium. As shown in Figure 3A (I and II), the extent of CVB3 infection was more pronounced in susceptible than resistant mice as also indicated by a higher viral load (A.BY/SnJ mice $8.6 \times 10^4 \pm 7 \times 10^4$/mg cardiac tissue versus C57BL/6 mice $4.2 \times 10^3 \pm 1 \times 10^3$/mg cardiac tissue at day 8 p.i.). However, individual cardiomyocytes of both mouse strains had similar CVB3 RNA levels (148 ± 10 grains/cell in A.BY/SnJ mice compared with 146 ± 11 grains/cell in C57BL/6 mice; $n = 50$ cells) when we enumerated the silver grains per cell. Specific LMP7 mRNA expression was detected not only in infiltrating immune cells within myocardial lesions but also in cardiomyocytes of infected susceptible and resistant mice compared with noninfected controls (compare Figure 3A, III and IV; V and VI). When we quantitated LMP7 mRNA expression levels in individual cells, we observed a significantly higher expression of LMP7 in infiltrating cells of susceptible A.BY/SnJ mice compared with resistant C57BL/6 mice (Figure 3B). In addition, LMP7 mRNA expression levels per cell were also significantly increased in cardiomyocytes of infected susceptible compared with resistant animals (Figure 3B). Grain density per cell was about eight times lower in cardiomyocytes compared with infiltrating cells, indicating higher LMP7 mRNA expression in inflammatory cells. These *in situ* hybridization results extend our microarray and real-time RT-PCR data by demonstrating increased immunoproteasome mRNA expression within cardiomyocytes and infiltrating immune cells independent of viral load. Moreover, quantification of signals on the single-cell level strongly indicates that the enhanced immunoproteasome mRNA expression in the hearts of susceptible animals is not merely due to increased viral load and subsequent enhanced infiltration of immune cells.

Enhanced Formation of Immunoproteasomes in CVB3-Infected Susceptible Mice

Having demonstrated increased RNA expression of immunoproteasomal subunits in CVB3-infected susceptible mice, we next sought to analyze whether these immunosubunits are translated and efficiently assembled into the 20S proteasome, thus forming the immunoproteasome. We purified 20S proteasomes from the myocardium of acutely CVB3-infected A.BY/SnJ and C57BL/6 mice and analyzed incorporation of immunoproteasomal subunits by Western blot and 2-D gel analysis. Western blot analysis of purified 20S proteasomes confirmed that the markedly increased mRNA levels of LMP2, LMP7, and MECL-1 in CVB3-infected A.BY/SnJ and C57BL/6 mice were translated and efficiently incorporated into the 20S proteasome (Figure 4, A and B). Importantly, the level of all three immunoproteasome subunits was clearly increased in the A.BY/SnJ mice compared with C57BL/6 mice (Figure 4, A and B), indicating enhanced incorporation of immunosubunits into 20S proteasomes of A.BY/SnJ mice. Purified immunoproteasomes and constitutive proteasomes from T27mp transfectant cells expressing the mouse proteasome subunits LMP2, MECL-1, and LMP7 in T2 cells (i20S) and nontransfected T2 cells (c20S) served as positive and negative controls, respectively (Figure 4A).[27] Expression of the constitutive 20S

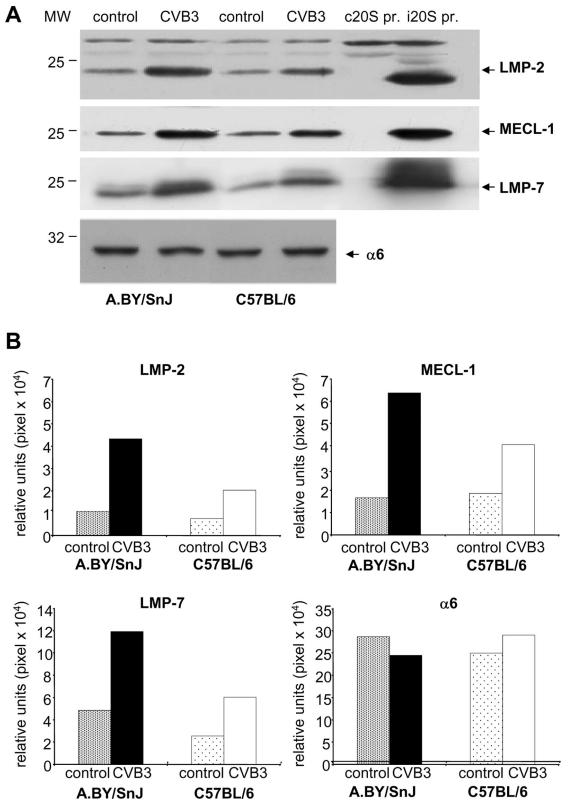

Figure 4. Enhanced incorporation of immunoproteasome subunits into 20S proteasomes of hearts of CVB3-infected resistant and susceptible mice. For purification of 20S proteasomes, 10 hearts of uninfected and CVB3-infected C57BL/6 and A.BY/SnJ mice were pooled, respectively, and Western blot analysis was performed. As controls, proteasomes of nontransfected T2 cells (c20S) and transfected T2 cells (i20S) were used. **A:** Purified 20S proteasomes from uninfected (control) or CVB3-infected mice were separated by SDS-PAGE and probed with specific antibodies to detect LMP2, MECL-1, LMP7, and α6 as indicated. Figure shows representative gel from two different 20S proteasome preparations. **B:** Densitometric analysis of the Western blot signals correspond to the indicated proteasome subunits in control and CVB3-infected mouse strains.

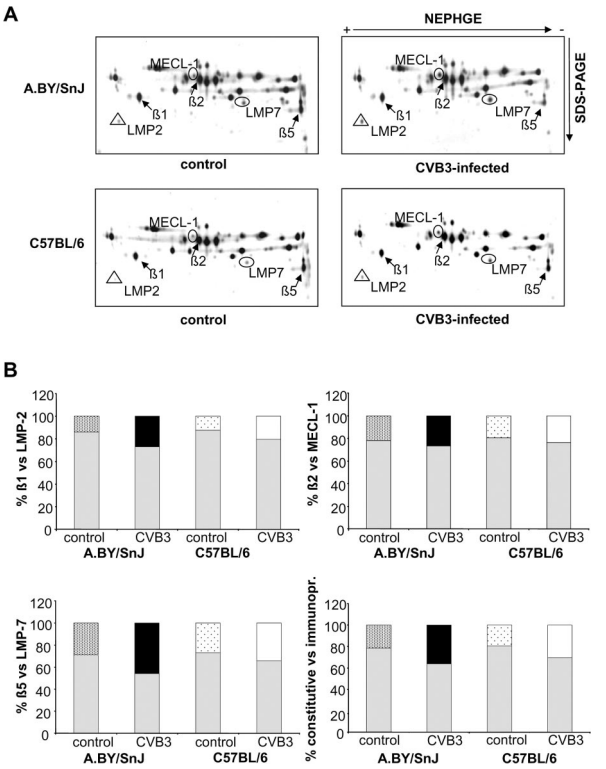

Figure 5. Two-dimensional IEF-SDS-PAGE of 20S proteasome purified from the pooled hearts of uninfected and CVB3-infected C57BL/6 and A.BY/SnJ mice. **A:** Purified 20S proteasomes from uninfected (**left**) or CVB3-infected (**right**) mice were separated by IEF-SDS-PAGE, and gels were silver stained. The **top panel** shows gels from A.BY/SnJ mice, the **bottom panel** from C57BL/6 mice. The constitutive subunits β1, β2, and β5 and the immunoproteasome subunits LMP2, LMP7, and MECL-1 are indicated. The 2-D gel patterns shown were reproducible in four gels of two independent 20S proteasome purifications. **B:** Densitometric evaluation of the indicated proteasome subunits (**A**). The intensity values of each corresponding pair of catalytic proteasome subunits are shown in single bars. In the fourth panel, bars represent percentage of combined constitutive β1, β2, and β5 subunits and of the immunosubunits LMP2, LMP7, and MECL-1.

proteasome subunit α6 was analyzed as a control for total proteasome expression. In both mouse strains, expression of α6 remained unaltered on CVB3 infection (Figure 4A), which is in accordance with real-time RT-PCR data (data not shown). Our results clearly show incorporation of immunosubunits into the 20S proteasome on CVB3 infection. Moreover, formation of immunoproteasomes is enhanced in mice susceptible to chronic myocarditis compared with resistant mice.

2-D Analysis of Immunosubunit Expression of 20S Proteasomes

To show that the differences in the expression of immunosubunits of the 20S proteasome are also reflected in the stochiometric subunit composition, purified 20S proteasomes from pooled hearts of uninfected and CVB3-infected mice were separated on IEF-SDS-PAGE two-dimensional gels followed by silver staining (Figure 5A). Proteasome subunits were assigned according to their migratory positions in 2-D gels as recently identified by matrix-assisted laser desorption-ionization mass spectrometry.[28] In uninfected myocardium, all immunoproteasome subunits were expressed at a low level compared with their constitutive counterparts. After CVB3 infection, incorporation of immunosubunits LMP2, LMP7, and MECL-1 into 20S proteasomes was significantly up-regulated during the acute phase of CVB3 myocarditis, whereas incorporation of the constitutive counterparts was concomitantly reduced as shown by quantitative densitometry (Figure 5B). Enhanced incorporation of immunoproteasome subunits was observed in CVB3-infected A.BY/SnJ mice compared with C57BL/6 animals (Figure 5, A and B). These data clearly indicate that CVB3-infected susceptible animals have higher levels of immunoproteasomes in the myocardium than infected resistant mice.

Altered Proteolytic Activities of the Proteasome in Hearts of CVB3-Infected Susceptible Mice

We next asked for the functional significance of immunoproteasome subunit incorporation into the proteasomes of CVB3-infected mice. Replacement of the three constitutive active subunits β1, β5, and β2 with LMP2, LMP7,

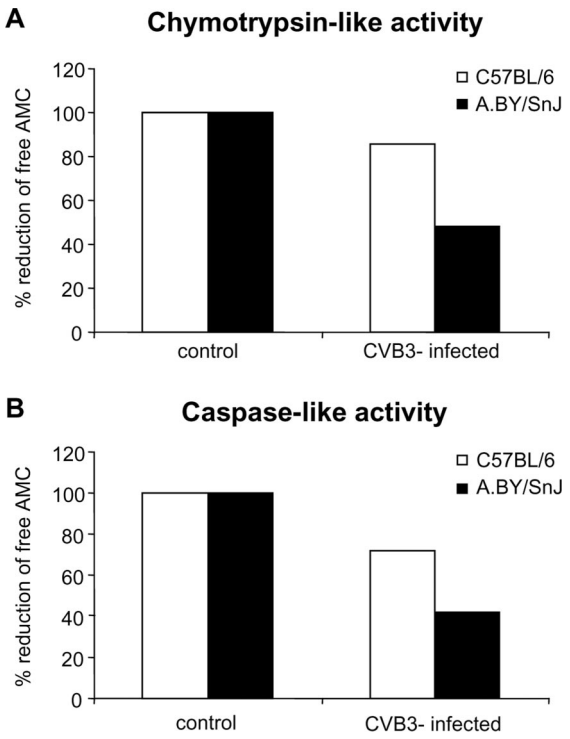

Figure 6. Altered proteolytic activities of purified heart proteasomes of CVB3-infected resistant and susceptible mice. Proteolytic activities of 20S proteasome purified from pooled hearts of uninfected and CVB3-infected A.BY/SnJ and C57BL/6 mice are depicted as percent reduction of free AMC. **A:** Chymotrypsin-like activity. **B:** Caspase-like activity.

and MECL-1 has been shown to affect the proteolytic activities of the proteasome, thereby altering quality and quantity of generated peptides.[27,29,30] Hence, we assayed the three main proteolytic activities, namely chymotrypsin-, caspase-, and trypsin-like, of purified cardiac 20S proteasomes of CVB3-infected and control mice (A.BY/SnJ, C57BL/6) *in vitro*.

The chymotryptic-like activity, which represents the main proteolytic activity of the constitutive proteasome, was clearly reduced in the hearts of CVB3-infected susceptible A.BY/SnJ mice compared with uninfected controls but to a lesser extent in C57BL/6 resistant mice (Figure 6A). 20S proteasomes from CVB3-infected mice also showed reduced caspase-like activities (Figure 6B). Again, this reduction was more pronounced in A.BY/SnJ than in C57BL/6 mice. The trypsin-like activities of the 20S proteasome were unaffected by CVB3 infection and did not differ between the mouse strains (data not shown). The alterations in proteolytic activities—reduction of chymotryptic- and caspase-like activities—corresponded to the enhanced incorporation of immunosubunits into the proteasomes on CVB3 infection and to increased levels of immunoproteasomes in susceptible A.BY/SnJ compared with resistant C57BL/6 mice. We observed a similar significant reduction in the chymotrypsin-like activity when we assayed whole-tissue lysates of the myocardium (data not shown). The reduction of constitutive proteasome activities points to an altered proteolytic activity by immunoproteasomes in the heart of CVB3-infected mice, an activity that is enhanced in susceptible compared with resistant mice.

Discussion

This study was undertaken to identify tissue-specific host factors that might influence the course of CVB3 infection in the susceptible and resistant host. Here, we provide evidence that susceptible mice, which develop ongoing myocarditis, express increased levels of immunoproteasomes and show altered proteasomal proteolytic activities during the acute phase of infection compared with resistant mice. This is accompanied by elevated levels of genes involved in the antigen-presenting machinery such as MHC class I molecules, β2-microglobulin, TAP, and tapasin.

To our knowledge, the data presented here are the first demonstrating increased immunoproteasome formation and activity in the myocardium after *in vivo* infection with CVB3, a human pathogenic enterovirus. Notably, the most prominent immunoproteasome expression was detected during the acute phase of infection, the time point when the specific T-cell response starts to evolve in the model of CVB3 myocarditis. Increased expression of LMP2 on cardiac infection with CVB3 has also been noted by a different microarray analysis.[31] Similar to our data, other *in vivo* models, including bacterial and fungal infections, demonstrate replacement of constitutive proteasomes by immunoproteasomes in the target organs at the onset of adaptive immunity, indicating that immunoproteasome formation and subsequent epitope generation influence the adaptive T-cell response to the infectious agent.[32–34] The most crucial finding of our study is that at the onset of acquired immunity, mice susceptible to ongoing myocarditis show increased immunoproteasome expression in cardiomyocytes and infiltrating cells compared with resistant mice.

On the basis of our data the following questions arise. First, does enhanced immunoproteasome formation in susceptible mice favor immune evasion of CVB3? Increased immunoproteasome formation was accompanied by enhanced expression of several genes involved in the antigen-presenting machinery, which indicates that CVB3 does not use the common viral escape strategy of MHC class I down-regulation.[35] There is also no evidence that any of the CVB3-encoded proteins act as ubiquitin ligases to enhance degradation of MHC class I molecules or to interfere directly with proteasome activity, which was observed for other viral infections.[36–39] The second question concerns the host response to CVB3: Does enhanced immunoproteasome formation affect quantity and quality of generated antigenic peptides, and what are the consequences for the specific CD8 T-cell response in CVB3 myocarditis? Fluorescence-activated cell sorting analysis revealed that the overall T-cell population in spleens of CVB3-infected animals at the acute phase was only slightly higher than in uninfected controls and that differences in $CD4^+$ and $CD8^+$ T-cell populations between susceptible and resistant mice were minimal ($CD4^+$ T cells 27.91 $\pm$ 0.86% in infected A.BY/SnJ

mice versus 21.07 ± 2.4% in C57BL/6 mice and for $CD8^+$ T cells 9.62 ± 0.62% versus 13.86 ± 0.64%, respectively).

Until now, we can only speculate on the answers concerning epitope-specific T cells because the antigenic epitopes generated by CVB3 are unknown, and no antigen-specific CD8 T-cell lines are yet available. In general, generation of MHC class I antigens is enhanced by immunoproteasomes, resulting in the improved presentation of immunodominant epitopes and concomitant changes in the specific CD8 T-cell repertoire.[40–47] Accordingly, increased formation of immunoproteasomes and enhanced expression of TAPs, tapasin, and MHC class I molecules in susceptible mice would result in improved formation and presentation of immunodominant epitopes and their corresponding T-cell clones. Surprisingly, up-regulation of the antigen-processing and -presenting machinery in susceptible mice does not lead to efficient virus elimination but results in increased immunopathology and ongoing myocarditis. One possible explanation could be exhaustion of immunodominant T cells after CVB3 infection as first described for chronic lymphocytic choriomeningitis virus infection by Zinkernagel.[48] Functional or physical exhaustion of immunodominant T cells has been observed during the acute phase of lymphocytic choriomeningitis virus infection, resulting in the reversion of immunodominance hierarchy, and exhaustion has been correlated with high levels of presented epitopes.[49] This hypothesis is also supported by findings that suboptimal immunoproteasome expression is sufficient to induce optimal CD8 T-cell activation.[42] According to this model, improved formation and presentation of immunodominant epitopes in susceptible mice might result in T-cell exhaustion, thereby resulting in incomplete virus elimination and persisting CVB3 infection in the myocardium. Alternative explanations could be that immunodominant epitopes generated by enhanced immunoproteasome activity are not protective, as shown for the M45 peptide in murine cytomegalovirus infection,[50] or that immunodominant epitopes may be generated less efficiently by immunoproteasomes of susceptible mice compared with resistant mice, as has been shown for some other viral and self epitopes.[51]

Yet, these hypotheses need to be verified. At present, it is unclear in which manner the proteasome affects generation of CVB3-derived antigenic peptides. Therefore, our future studies will focus on the processing and generation of MHC class I-restricted epitopes of CVB3 polypeptides by the proteasome and on the establishment of CVB3 antigen-specific CD8 T cells to decipher the specific CD8 T-cell response of the resistant and susceptible host.

The present study may be of value to understand persisting viral infections in general and persisting CVB3 infections in particular. In light of the rising evidence that cardiotropic viruses are prevalent environmental factors that may cause or modulate the course of dilated cardiomyopathy, our study may contribute to improving diagnosis and prognosis of patients susceptible for the development of ongoing myocarditis and dilated cardiomyopathy.

Acknowledgments

We are grateful for the superb technical assistance of Sabine Schäfer, Andrea Weller, and Kornelia Buttke. We thank the lab of Dr. Peter Jungblut (Max-Planck-Institute of Infectious Biology, Berlin) for performing the 2-D electrophoresis and Dr. K. Janek (Institute of Biochemistry, Charité-Universitätsmedizin) for identification of proteins by mass spectrometry.

References

1. Mason JW: Myocarditis and dilated cardiomyopathy: an inflammatory link. Cardiovasc Res 2003, 60:5–10
2. Kuehl U, Pauschinger M, Noutsias M, Seeberg B, Bock T, Lassner D, Poller W, Kandolf R, Schultheiss HP: High prevalence of viral genomes and multiple viral infections in the myocardium of adults with "idiopathic" left ventricular dysfunction. Circulation 2005, 111:887–893
3. Huber SA, Gauntt CJ, Sakkinen P: Enteroviruses and myocarditis: viral pathogenesis through replication, cytokine induction, and immunopathogenicity. Adv Virus Res 1998, 51:35–80
4. Klingel K, Sauter M, Bock CT, Szalay G, Schnorr JJ, Kandolf R: Molecular pathology of inflammatory cardiomyopathy. Med Microbiol Immunol 2004, 193:101–107
5. Klingel K, Hohenadl C, Canu A, Albrecht M, Seemann M, Mall G, Kandolf R: Ongoing enterovirus-induced myocarditis is associated with persistent heart muscle infection: quantitative analysis of virus replication, tissue damage, and inflammation. Proc Natl Acad Sci USA 1992, 89:314–318
6. Chow LH, Beisel KW, McManus BM: Enteroviral infection of mice with severe combined immunodeficiency: evidence for direct viral pathogenesis of myocardial injury. Lab Invest 1992, 66:24–31
7. Mena I, Perry CM, Harkins S, Rodriguez F, Gebhard J, Whitton JL: The role of B lymphocytes in coxsackievirus B3 infection. Am J Pathol 1999, 155:1205–1215
8. Kandolf R, Ameis D, Kirschner P, Canu A, Hofschneider PH: In situ detection of enteroviral genomes in myocardial cells by nucleic acid hybridization: an approach to the diagnosis of viral heart disease. Proc Natl Acad Sci USA 1987, 84:6272–6276
9. Henke A, Huber S, Stelzner A, Whitton JL: The role of CD8+ T lymphocytes in coxsackievirus B3-induced myocarditis. J Virol 1995, 69:6720–6728
10. Leipner C, Borchers M, Merkle I, Stelzner A: Coxsackievirus B3-induced myocarditis in MHC class II-deficient mice. J Hum Virol 1999, 2:102–114
11. Klingel K, Schnorr JJ, Sauter M, Szalay G, Kandolf R: Beta2-microglobulin-associated regulation of interferon-gamma and virus-specific immunoglobulin G confer resistance against the development of chronic coxsackievirus myocarditis. Am J Pathol 2003, 162:1709–1720
12. Gebhard JR, Perry CM, Harkins S, Lane T, Mena I, Asensio VC, Campbell IL, Whitton JL: Coxsackievirus B3-induced myocarditis: perforin exacerbates disease, but plays no detectable role in virus clearance. Am J Pathol 1998, 153:417–428
13. Huber SA, Mortensen A, Moulton G: Modulation of cytokine expression by CD4+ T cells during coxsackievirus B3 infections of BALB/c mice initiated by cells expressing the gamma delta + T-cell receptor. J Virol 1996, 70:3039–3044
14. Wong P, Pamer EG: CD8 T cell responses to infectious pathogens. Annu Rev Immunol 2003, 21:29–70
15. Kloetzel PM: Antigen processing by the proteasome. Nat Rev Mol Cell Biol 2001, 2:179–187
16. Voges D, Zwickl P, Baumeister W: The 26S proteasome: a molecular machine designed for controlled proteolysis. Annu Rev Biochem 1999, 68:1015–1068
17. Boes B, Hengel H, Ruppert T, Multhaup G, Koszinowski UH, Kloetzel PM: Interferon gamma stimulation modulates the proteolytic activity and cleavage site preference of 20S mouse proteasomes. J Exp Med 1994, 179:901–909
18. Kloetzel PM, Ossendorp F: Proteasome and peptidase function in

MHC-class-I-mediated antigen presentation. Curr Opin Immunol 2004, 16:76–81
19. Kandolf R, Hofschneider PH: Molecular cloning of the genome of a cardiotropic coxsackie B3 virus: full-length reverse-transcribed recombinant cDNA generates infectious virus in mammalian cells. Proc Natl Acad Sci USA 1985, 2:4818–4822
20. Meiners S, Heyken D, Weller A, Ludwig A, Stangl K, Kloetzel PM, Kruger E: Inhibition of proteasome activity induces concerted expression of proteasome genes and de novo formation of mammalian proteasomes. J Biol Chem 2003, 278:21517–21525
21. Kuckelkorn U, Ferreira EA, Drung I, Liewer U, Kloetzel PM, Theobald M: The effect of the interferon-gamma-inducible processing machinery on the generation of a naturally tumor-associated human cytotoxic T lymphocyte epitope within a wild-type and mutant p53 sequence context. Eur J Immunol 2002, 32:1368–1375
22. Klose J, Kobalz U: Two-dimensional electrophoresis of proteins: an updated protocol and implications for a functional analysis of the genome. Electrophoresis 1995, 16:1034–1059
23. Jungblut PR, Seifert R: Analysis by high-resolution two-dimensional electrophoresis of differentiation-dependent alterations in cytosolic protein pattern of HL-60 leukemic cells. J Biochem Biophys Methods 1990, 21:47–58
24. Lamer S, Jungblut PR: Matrix-assisted laser desorption-ionization mass spectrometry peptide mass fingerprinting for proteome analysis: identification efficiency after on-blot or in-gel digestion with and without desalting procedures. J Chromatogr B Biomed Sci Appl 2001, 752:311–322
25. Griffin TA, Nandi D, Cruz M, Fehling HJ, Van Kaer L, Monaco JJ, Colbert RA: Immunoproteasome assembly: cooperative incorporation of interferon gamma (IFN-γ)-inducible subunits. J Exp Med 1998, 187:97–104
26. Princiotta MF, Finzi D, Qian SB, Gibbs J, Schuchmann S, Buttgereit F, Bennink JR, Yewdell JW: Quantitating protein synthesis, degradation, and endogenous antigen processing. Immunity 2003, 3:343–354
27. Kuckelkorn U, Frentzel S, Kraft R, Kostka S, Groettrup M, Kloetzel PM: Incorporation of major histocompatibility complex-encoded subunits LMP2 and LMP7 changes the quality of the 20S proteasome polypeptide processing products independent of interferon-gamma. Eur J Immunol 1995, 25:2605–2611
28. Kuckelkorn U, Ruppert T, Strehl B, Jungblut PR, Zimny-Arndt U, Lamer S, Prinz I, Drung I, Kloetzel PM, Kaufmann SH, Steinhoff U: Link between organ-specific antigen processing by 20S proteasomes and CD8(+) T cell-mediated autoimmunity. J Exp Med 2002, 195:983–990
29. Eleuteri AM, Kohanski RA, Cardozo C, Orlowski M: Bovine spleen multicatalytic proteinase complex (proteasome): replacement of X, Y, and Z subunits by LMP7, LMP2, and MECL1 and changes in properties and specificity. J Biol Chem 1997, 272:11824–11831
30. Toes RE, Nussbaum AK, Degermann S, Schirle M, Emmerich NP, Kraft M, Laplace C, Zwinderman A, Dick TP, Muller J, Schonfisch B, Schmid C, Fehling HJ, Stevanovic S, Rammensee HG, Schild H: Discrete cleavage motifs of constitutive and immunoproteasomes revealed by quantitative analysis of cleavage products. J Exp Med 2001, 194:1–12
31. Taylor LA, Carthy CM, Yang D, Saad K, Wong D, Schreiner G, Stanton LW, McManus BM: Host gene regulation during coxsackievirus B3 infection in mice: assessment by microarrays. Circ Res 2002, 87:328–334
32. van den Eynde BJ, Morel S: Differential processing of class-I-restricted epitopes by the standard proteasome and the immunoproteasome. Curr Opin Immunol 2001, 13:147–153
33. Khan S, van den Broek M, Schwarz K, de Giuli R, Diener PA, Groettrup M: Immunoproteasomes largely replace constitutive proteasomes during an antiviral and antibacterial immune response in the liver. J Immunol 2001, 167:6859–6868
34. Barton LF, Cruz M, Rangwala R, Deepe GS Jr, Monaco JJ: Regulation of immunoproteasome subunit expression in vivo following pathogenic fungal infection. J Immunol 2002, 169:3046–3052
35. Alcami A, Koszinowski U: Viral mechanisms of immune evasion. Immunol Today 2000, 21:447–455
36. Boname JM, Stevenson PG: MHC class I ubiquitination by a viral PHD/LAP finger protein. Immunity 2001, 15:627–6361
37. Liu Y-C: Ubiquitin ligases and the immune system. Annu Rev Immunol 2004, 22:81–127
38. Rivett AJ, Hearn AR: Proteasome function in antigen presentation: immunoproteasome complexes, peptide production, and interactions with viral proteins. Curr Protein Pept Sci 2004, 5:153–161
39. Luo H, Zhang J, Cheung C, Suarez A, McManus BM, Yang D: Proteasome inhibition reduces coxsackievirus B3 replication in murine cardiomyocytes. Am J Pathol 2003, 163:381–385
40. Van Kaer L, Ashton-Rickardt PG, Eichelberger M, Gaczynska M, Nagashima K, Rock KL, Goldberg AL, Doherty PC, Tonegawa S: Altered peptidase and viral-specific T cell response in LMP2 mutant mice. Immunity 1994, 1:533–541
41. Eggers M, Boes-Fabian B, Ruppert T, Kloetzel PM, Koszinowski UH: The cleavage preference of the proteasome governs the yield of antigenic peptides. J Exp Med 1995, 182:1865–1870
42. Sijts AJ, Ruppert T, Rehermann B, Schmidt M, Koszinowski U, Kloetzel PM: Efficient generation of a hepatitis B virus cytotoxic T lymphocyte epitope requires the structural features of immunoproteasomes. J Exp Med 2000, 191:503–514
43. Sijts AJ, Standera S, Toes RE, Ruppert T, Beekman NJ, van Veelen PA, Ossendorp FA, Melief CJ, Kloetzel PM: MHC class I antigen processing of an adenovirus CTL epitope is linked to the levels of immunoproteasomes in infected cells. J Immunol 2000, 164:4500–4506
44. Schwarz K, van den Broek M, Kostka S, Kraft R, Soza A, Schmidtke G, Kloetzel PM, Groettrup M: Overexpression of the proteasome subunits LMP2, LMP7, and MECL-1, but not PA28 alpha/beta, enhances the presentation of an immunodominant lymphocytic choriomeningitis virus T cell epitope. J Immunol 2000, 165:768–778
45. van Hall T, Sijts A, Camps M, Offringa R, Melief C, Kloetzel PM, Ossendorp F: Differential influence on cytotoxic T lymphocyte epitope presentation by controlled expression of either proteasome immunosubunits or PA28. J Exp Med 2000, 192:483–494
46. Chen W, Norbury CC, Cho Y, Yewdell JW, Bennink JR: Immunoproteasomes shape immunodominance hierarchies of antiviral CD8(+) T cells at the levels of T cell repertoire and presentation of viral antigens. J Exp Med 2001, 193:1319–1326
47. Basler M, Youhnovski N, van den Broek M, Przybylski M, Groettrup M: Immunoproteasomes down-regulate presentation of a subdominant T cell epitope from lymphocytic choriomeningitis virus. J Immunol 2004, 173:3925–3934
48. Moskophidis D, Lechner F, Pircher H, Zinkernagel RM: Virus persistence in acutely infected immunocompetent mice by exhaustion of antiviral cytotoxic effector T cells. Nature 1993, 362:758–761
49. Wherry EJ, Blattman JN, Murali-Krishna K, van der Most R, Ahmed R: Viral persistence alters CD8 T-cell immunodominance and tissue distribution and results in distinct stages of functional impairment. J Virol 2003, 77:4911–4927
50. Holtappels R, Podlech J, Pahl-Seibert MF, Julch M, Thomas D, Simon CO, Wagner M, Reddehase MJ: Cytomegalovirus misleads its host by priming of CD8 T cells specific for an epitope not presented in infected tissues. J Exp Med 2004, 199:131–136
51. Morel S, Levy F, Burlet-Schiltz O, Brasseur F, Probst-Kepper M, Peitrequin AL, Monsarrat B, Velthoven R, Cerottini JC, Boon T, Gairin JE, van den Eynde BJ: Processing of some antigens by the standard proteasome but not by the immunoproteasome results in poor presentation by dendritic cells. Immunity 2000, 12:107–117